USCAP

Check for updates

ARTICLE

Long non-coding RNA MALAT1 enhances angiogenesis during bone regeneration by regulating the miR-494/SP1 axis

Ao Ding[1], Cheng-Hua Li[2], Chan-Yuan Yu[1], Hang-Tian Zhou[1] and Zhi-Hong Zhang [1]✉

Bone regeneration is a coordinated process involving connections between blood vessels and osteocytes. Angiogenesis and osteogenesis are tightly connected throughout the progression of bone regeneration. This study aimed to explore the underlying mechanism of metastasis-associated lung adenocarcinoma transcript 1 (MALAT1)-regulated angiogenesis during bone regeneration. Gene and protein expression was detected by quantitative real-time PCR and western blot assay. Vascular endothelial growth factor (VEGFA) secretion was assessed by enzyme-linked immunosorbent assay. To evaluate the effect of osteogenic differentiation, alkaline phosphatase (ALP) and alizarin red staining assays were performed. Proliferation was detected by 3-(4,5-Dimethylthiazol-2-yl)-2,5-diphenyltetrazolium bromide assay. Migration and angiogenesis were measured using Transwell and tube formation assays. A dual luciferase reporter assay was performed to confirm the binding relationship among MALAT1, miR-494, and specificity protein 1 (SP1). Expression levels of MALAT1, SP1, and VEGFA were elevated and miR-494 was suppressed in MC3T3-E1 cells after culture in osteogenic medium. MALAT1 knockdown suppressed the osteogenic differentiation of MC3T3-E1, since ALP activity, mineralized nodules, and expression of the osteodifferentiated markers runt-related transcription factor 2 and osterix were restrained. In addition, MALAT1 silencing inhibited angiogenesis during bone regeneration, as the proliferation, migration, and capillary tube formation of human umbilical vein endothelial cells were blocked. Furthermore, miR-494 was directly targeted by MALAT1 and regulated the SP1/Toll-like receptor 2 (TLR2)/bone morphogenetic protein 2 (BMP2) axis by targeting SP1. Furthermore, miR-494 overexpression inhibited angiogenesis and osteogenic differentiation. Moreover, SP1 overexpression or miR-494 inhibition rescued the regulatory effect of sh-MALAT1 on angiogenesis and osteogenic differentiation. Taken together, these findings indicate that MALAT1 promotes angiogenesis and osteogenic differentiation by targeting miR-494 and activating the SP1/TLR2/BMP2 pathway, suggesting a novel target for bone regeneration therapy by promoting angiogenesis.

INTRODUCTION

Bone tissue maintains the homeostasis and integrity of the body through continuous bone resorption and bone formation that together comprise bone regeneration[1]. Both bone metabolism and bone defect repair are achieved by relying on bone regeneration[2]. However, the repair and reconstruction of large segmental bone defects induced by trauma, cancer, and infection remain a significant challenge[3]. During the progression of bone regeneration, blood vessels are not only involved in the transportation of circulating stem cells (CSCs), oxygen, nutrients, and metabolites but also generate vascular secretion factors involved in bone growth and homeostasis[4]. Angiogenesis and osteogenesis are closely related throughout the progression of bone regeneration[5]. Therefore, there is an urgent need to improve our understanding of the molecular mechanisms that drive angiogenesis during bone regeneration to identify improved therapeutic options.

Long non-coding RNAs (lncRNAs), which are more than 200 nucleotides in length, have recently been identified as key regulators in a series of biological functions, such as gene expression, cell proliferation, and differentiation[6]. Increasing evidence has revealed that lncRNAs play an important role in the regulation of angiogenesis[7,8] and osteogenic differentiation[9]. Moreover, lncRNA maternally expressed gene 3 is uncovered to be involved in osteoarthritis development via the regulation of angiogenesis[10]. LncRNA metastasis-associated lung adenocarcinoma transcript 1 (MALAT1) is revealed to regulate angiogenesis in microvascular endothelial cells and gastric cancer[6,11], promoting osteogenic differentiation[12]. However, whether MALAT1 is involved in angiogenesis during bone regeneration is still unknown.

MicroRNAs (miRNAs) are endogenous, small, non-coding RNAs of ~22 nucleotides that negatively modulate target genes by suppressing translation and improving mRNA recession[13]. MiRNAs have been identified as important regulators of bone regeneration and angiogenesis[14–16]. MiR-494 is inhibited during bone regeneration and angiogenesis, and overexpression of miR-494 reduces osteogenic differentiation gene expression[14,17]. However, whether miR-494 participates in the progression of angiogenesis in bone regeneration remains unknown, and the mechanism requires deep investigation.

[1]Department of Stomatology, The First Affiliated Hospital of USTC (Anhui Provincial Hospital), Division of Life Sciences and Medicine, University of Science and Technology of China, Hefei, Anhui Province, P.R. China. [2]Department of Stomatology, Beidaihe Rihabilitation and Recuperation Center of PLA, Qinhuangdao, Hebei Province, P.R. China. ✉email: zhangzhihong769@163.com

Transcription factor specificity protein 1 (SP1) is a member of the Sp transcription factor family[18]. SP1 is highly related to tumors, angiogenesis, differentiation, and other physiological and pathological processes[18–20]. Recent evidence confirmed that SP1 enhances tumor angiogenesis and invasion by enhancing vascular endothelial growth factor (VEGF) in ovarian cancer[20]. TLR2, a crucial member of the family of Toll-like receptors (TLRs), has recently been defined to be related to angiogenesis and bone repair[21,22]. Moreover, TLR2 activation dramatically upregulates the expression of hypoxia-inducible factor-1α (HIF-1α) and bone morphogenetic protein 2 (BMP2), stimulating bone mesenchymal stem cell (BMSC)-mediated angiogenesis and osteogenesis[23]. In addition, several studies reported that SP1 regulates TLR2 promoter activity in atherosclerosis[24]; therefore, we hypothesized that the SP1/TLR2/BMP2 signaling pathway might play a role in angiogenesis in bone regeneration. In addition, MALAT1 was shown to promote SP1 by direct interaction[19]. In this study, we explored whether MALAT1 modulated bone regeneration by regulating the SP1/TLR2/BMP2 signaling pathway.

In this study, we found that MALAT1 promotes angiogenesis during bone regeneration through activation of the SP1/TLR2/BMP2 signaling pathway by targeting miR-494. These findings suggest a novel signaling axis, comprising MALAT1-miR-494-SP1/TLR2/BMP2, in the regulation of angiogenesis in bone regeneration, providing a potential target for bone regeneration.

MATERIALS AND METHODS
Cell culture
Mouse osteoblastic MC3T3-E1 cells and human umbilical vein endothelial cells (HUVECs) were obtained from the Cell Bank of the Chinese Academy of Sciences (Shanghai, China). MC3T3-E1 cells were cultured in α-MEM (Sigma-Aldrich, USA), and HUVECs were maintained in Dulbecco's modified Eagle's medium (Sigma-Aldrich) with 10% fetal bovine serum (FBS, HyClone, USA) and 100 U/mL penicillin and 100 μg/mL streptomycin. Cells were incubated in a humidified atmosphere with 5% CO_2 at 37 °C. For osteogenic differentiation, MC3T3-E1 cells were cultured in osteogenic medium (α-MEM, 10% FBS, 1% penicillin/streptomycin, 50 μg/mL L-ascorbic acid, 10 mM glycerophosphate, and 100 nM dexamethasone) for 5, 10, or 15 days.

Cell transfection
MC3T3-E1 cells (2×10^5) were plated into six-well plates. MiR-494 mimics and SP1 overexpression were induced by transfection of plasmids using the Lipofectamine 2000 reagent (Invitrogen, USA). For short hairpin RNA (shRNA) experiments, MC3T3-E1 cells were introduced into shRNA with jetPRIME® (Polyplus, USA). The lentiviral shRNA vector pLKO.1-puro (SHC001) was obtained from Sigma-Aldrich. MALAT1-shRNA (sequence: 5′-CACAGGGAAAGCGAGTGGTTGGTAA-3′) was obtained from Sigma-Aldrich.

Luciferase assay
The luciferase reporter assay was performed as previously reported[25,26]. MC3T3-E1 cells were plated into 96-well plates at 5000 cells per well. Sequences containing wild-type, mutant MALAT1 or SP1 functional sites were synthesized (Sangon Biotech, Shanghai) and inserted into the pmirGLO Dual-Luciferase Target Expression Vector (Promega Corporation, Madison, WI, USA). The cells were transfected with miR-494 mimics or mimics NC with Lipofectamine 2000. After 48 h, each value from the firefly luciferase assay was normalized to the Renilla luciferase assay value.

Quantitative real-time PCR (qRT-PCR)
Total RNA was isolated from MC3T3-E1 cells using TRIzol® reagent (Invitrogen), and the concentration of total RNA was determined using a microplate absorbance reader (Bio-Rad Model 680) and dissolved in diethyl pyrocarbonate water. Then, cDNA was synthesized using reverse transcription. Real-time PCR was conducted using the SYBR Premix Ex Taq Kit (TaKaRa, Japan). The amplification conditions were as follows: 95 °C for 10 min to activate the polymerization reaction, followed by 40 cycles of 10 s at 95 °C, 15 s at 60 °C, and 10 s at 72 °C. Relative expression levels were

calculated using the $2^{-\Delta\Delta Ct}$ method. The primer sequences for qRT-PCR were as follows:

MALAT1-F: 5′-GTATGTAGGCCTTTGCGGGT-3′,
MALAT1-R: 5′-GGTTGTGCTGGCTCTACCAT-3′,
miR-494-F: 5′-GTTGGCTCTGGTGCAGGGTCCGAGGTATTCGCACCAGAGC-CAACGAGGTT-3′,
miR-494-R: 5′-GGCTGAAACATACACGGGA-3′,
SP1-F: 5′-TGGGTACTTCAGGGATCCAG-3′,
SP1-R: 5′-TGAGGCTCTTCCCTCACTGT-3′,
U6-F: 5′-CTCGCTTCGGCAGCACA-3′,
U6-R: 5′-AACGCTTCACGAATTTGCGT-3′,
GAPDH-F: 5′-AGCCCAAGATGCCCTTCAGT-3′,
GAPDH-R: 5′-CCGTGTTCCTACCCCCAATG-3′.

Enzyme-linked immunosorbent assay (ELISA)
The release of VEGFA was detected using an ELISA kit (Thermo Fisher Scientific, Inc.) according to the manufacturer's instructions. We used the supernatant of MC3T3-E1 cells for the VEGFA ELISA. In short, samples mixed with diluent buffers were provided at a ratio of 1:1. Then, we added 100 μL of mixed samples per well to a 96-well plate. The plate was incubated at 4 °C overnight. After incubation, the plate was washed and incubated with biotin conjugate at room temperature for 1 h. We then added 100 μL streptavidin-horseradish peroxidase (HRP) to each well, and the plate was then incubated at room temperature in the dark. Plates were subsequently washed, and each well was incubated with 100 μL stabilized chromogen for 30 min at room temperature in the dark. We then added 100 μL stop solution to each well, and the optical density was determined at a wavelength of 450 nm (Bio-Rad Model 680).

Alkaline phosphatase (ALP) activity assay
ALP activity was determined using an ALP Assay kit (Beijing Baiaolaibo Biotechnology, Beijing, China) according to the manufacturer's instructions. MC3T3-E1 cells were lysed using lysis buffer in 96 plates and then incubated at 37 °C for 30 min. Then, 100 μL termination solution was added to each well, and the supernatant was assessed by a microplate absorbance reader at 405 nm (Bio-Rad Model 680).

Alizarin red staining (ARS) assay
ARS assay was performed as previously reported[27]. MC3T3-E1 cells were fixed in 10% precooled paraformaldehyde for 20 min and then washed with PBS three times. Next, the cells were stained with 40 mmol/L ARS solution (Sigma-Aldrich) for 15 min at room temperature. After staining, MC3T3-E1 cells were washed and subsequently dried and photographed.

Western blotting
MC3T3-E1 cells were lysed in radio immunoprecipitation assay lysis buffer. The concentration of protein was detected using a protein quantification kit (BCA Assay, Pierce, USA). Protein extracts were resolved by 8–10% sodium dodecyl sulfate-polyacrylamide gel electrophoresis gel electrophoresis and transferred onto polyvinylidene fluoride membranes (Millipore, USA). Then, the membranes were blocked in 5% non-fat milk and incubated at 4 °C overnight with primary antibodies. Primary antibodies specific to SP1, TLR2, BMP2, runt-related transcription factor 2 (RUNX2), and osterix (OSX) were purchased from Cell Signaling Technology (Boston, USA). The membranes were washed and then incubated with the corresponding HRP-conjugated secondary antibodies and electrochemiluminescence detection reagent (Amersham Biosciences, Australia) to visualize the proteins using an AI600 (GE Healthcare, USA). Glyceraldehyde-3-phosphate dehydrogenase was used as an internal reference.

3-(4,5-Dimethylthiazol-2-yl)-2,5-diphenyltetrazolium bromide (MTT) assay
Cells with or without transfection were plated into 96-well plates at 10,000 cells per well. After 48 h, 20 μL MTT stock solution (5 mg/mL) was added for 4 h. Then, we used dimethyl sulfoxide to dissolve the formazan (200 μL per well), and optical density values were detected at 490 nm.

Transwell assay
The migratory capability of HUVECs was detected using a Transwell assay. A total of 2×10^5 cells were seeded onto Matrigel-coated membranes in the upper compartment. After 24 h, migrated cells were fixed and stained with methylene blue. Cells were imaged, and the total numbers of
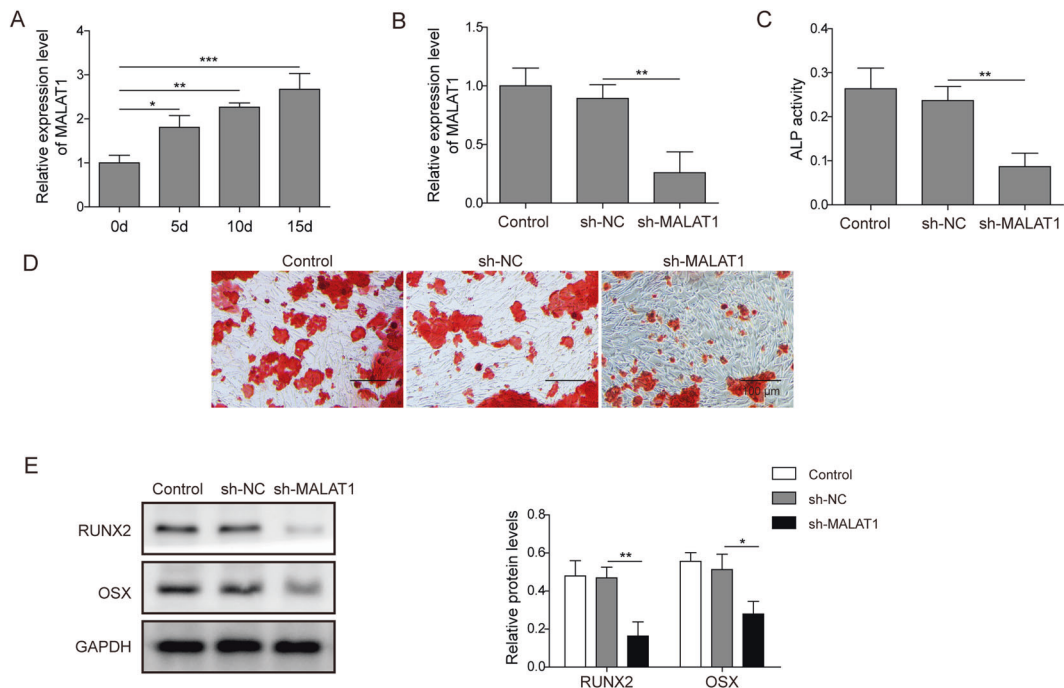
Fig. 1 Osteogenic differentiation is suppressed in response to silencing MALAT1. A MC3T3-E1 cells were cultured in osteogenic medium for 5, 10, or 15 days, and levels of MALAT1 were evaluated by qRT-PCR. **B–E** MC3T3-E1 cells were transfected with sh-MALAT1 or control shRNA. **B** Levels of MALAT1 were detected by qRT-PCR. **C** The activity of ALP was detected using an ALP detection kit. **D** ARS assay was determined to assess mineralized nodules. **E** Protein expression of RUNX2 and OSX was determined by western blot assay. Data are the mean ± SD of three separate experiments. The P value was determined by ANOVA following Tukey's post hoc test or Student's t-test. *$P < 0.05$, **$P < 0.01$, and ***$P < 0.001$.

migrated cells were quantified by counting using an inverted light microscope (Olympus, Long Island, NY).

Tube formation assay
HUVECs (2×10^4 per well) were plated into 12-well plates coated with Matrigel Basement Membrane Matrix (BD Bioscience) and incubated for 6 h. Four areas of each sample were imaged, and we counted the number of tube branches three times. Any increase or decrease in the formation of tubes compared to control wells indicates changes in angiogenic or antiangiogenic function, respectively.

Statistical analysis
We used GraphPad Prism version 5.0 software (GraphPad Software, Inc.), and data are presented as the mean ± standard deviation (SD) from three independent tests. Significant differences between groups were determined by Student's t-test or one-way ANOVA followed by Tukey's post hoc test for multiple comparisons. A statistically significant difference was defined as $P < 0.05$.

RESULTS
MALAT1 knockdown suppresses the osteogenic differentiation of MC3T3-E1 cells
Since MALAT1 was reported to participate in the progression of osteogenic differentiation[12], we examined the role of MALAT1 in bone regeneration. As shown in Fig. 1A, MALAT1 expression levels in MC3T3-E1 cells were elevated in response to osteogenic medium in a time-dependent manner. To further investigate whether MALAT1 triggers osteogenic differentiation, we introduced control and MALAT1 shRNA lentiviruses into MC3T3-E1 cells. The efficiency of MALAT1 silencing is shown in Fig. 1B. As expected, ALP activity in MALAT1 knockdown cells was reduced compared to that in the control group (Fig. 1C). Similar results were observed in the ARS staining assay, in which knockdown of MALAT1 markedly inhibited matrix mineralization (Fig. 1D). Moreover, we utilized western blot assays to evaluate expression of the

osteogenic-associated proteins RUNX2 and OSX. Remarkably, treatment with MALAT1 shRNA inhibited the expression of both RUNX2 and OSX (Fig. 1E). In conclusion, the above results indicate that MALAT1 is upregulated in osteogenic cells and that MALAT1 depletion blocks osteogenic differentiation in MC3T3-E1 cells.

Knockdown of MALAT1 restrains angiogenesis in vitro
It is well known that angiogenesis is highly related to osteogenesis during the progression of bone regeneration; therefore, we examined whether MALAT1 influences angiogenesis during osteogenic differentiation of MC3T3-E1 cells. ELISA was performed to measure the concentration of the angiogenesis-related factor VEGFA in the culture medium of MC3T3-E1 cells. Consistent with our hypothesis, we found that secretion of VEGFA was significantly enhanced in MC3T3-E1 cells in a time-dependent manner in osteogenic medium (Fig. 2A). Moreover, MALAT1 silencing significantly decreased the VEGFA concentration (Fig. 2B), indicating that VEGFA is elicited during the progression of osteogenic differentiation. Furthermore, we treated HUVECs with the supernatant of MC3T3-E1 cells transfected with sh-MALAT1 or sh-NC. As shown in Fig. 2C, MALAT1 knockdown markedly inhibited the proliferation of HUVECs, as examined by MTT assay. In addition, Transwell assays indicated that silencing MALAT1 significantly diminished the migration of HUVECs (Fig. 2D). To explore the roles of MALAT1 in angiogenesis, a tube formation assay was performed to detect angiogenic potency. As shown in Fig. 2E, MALAT1 shRNA abolished the well-organized, capillary-like networks compared to the control group. Overall, we demonstrate that knockdown of MALAT1 restrains angiogenesis in vitro.

MALAT1 mediates the SP1/TLR2/BMP2 axis by targeting miR-494
LncRNAs interact with miRNAs as competitive endogenous RNAs, participating in the regulation of target gene expression. To understand the mechanism by which MALAT1 regulates
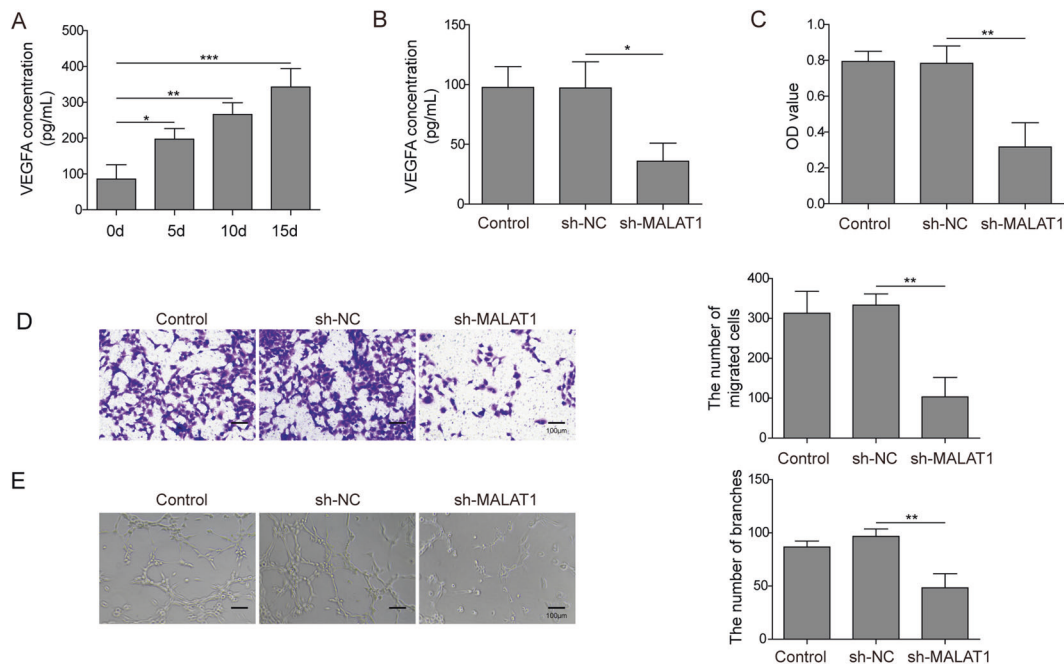
Fig. 2 Knockdown of MALAT1 represses angiogenesis in vitro. A MC3T3-E1 cells were treated with osteogenic medium for 5, 10, or 15 days. VEGFA concentration in the supernatant was evaluated by ELISA. **B** The VEGFA concentration of MC3T3-E1 cells transfected with or without MALAT1 shRNA in the supernatant was evaluated by ELISA. **C–E** HUVECs were treated with the supernatant from MC3T3-E1 cells transfected with MALAT1 knockdown or control shRNA. **C** Proliferation of HUVECs was detected using the MTT assay. **D** Migration of HUVECs was measured by Transwell assay. **E** Tube formation of HUVECs was observed under a microscope, and an image of each well is shown. Data are the mean ± SD for three separate experiments. The *P* value was determined by ANOVA following Tukey's post hoc test or Student's *t*-test. *$P < 0.05$, **$P < 0.01$, and ***$P < 0.001$.

angiogenesis and osteogenic differentiation, we investigated the downstream targets of MALAT1-miR-494 and how to modulate angiogenesis and osteogenic differentiation. As shown in Fig. 3A, we observed a potential binding site between MALAT1 and miR-494. In addition, we discovered that the transcription factor SP1 has a potential binding site with miR-494 using bioinformatics methods. To verify the predicted results, a dual luciferase reporter assay was performed, and the results showed that miR-494 mimics inhibited luciferase activity in the MALAT1-wild type (MALAT1-WT) and SP1-WT groups but not in the MALAT1-mutant (MALAT1-MUT) and SP1-MUT groups (Fig. 3B). To further explore whether MALAT1 acts as a sponge of miR-494, we interfered with MALAT1 expression in MC3T3-E1 cells. As expected, silencing MALAT1 markedly promoted the expression of miR-494 (Fig. 3C). Next, we explored whether SP1 was modulated by the MALAT1-miR-494 axis. qRT-PCR results indicated that overexpression of miR-494 significantly blocked SP1 mRNA levels, while inhibition of miR-494 activated SP1 expression. SP1 expression was suppressed by sh-MALAT1 (Fig. 3D). Moreover, western blotting also demonstrated that miR-494 mimics reduced the expression of SP1 and its downstream proteins TLR2 and BMP2; however, the miR-494 inhibitor displayed the opposite effect (Fig. 3E). Taken together, these data reveal that MALAT1 activates the SP1/TLR2/BMP2 signaling axis by directly targeting miR-494.

Overexpression of miR-494 inhibits osteogenic differentiation and angiogenesis in MC3T3-E1 cells

To explore the function of miR-494 in osteogenic differentiation and angiogenesis, qRT-PCR assays were performed, and the results revealed that osteogenic medium decreased miR-494 expression in a dose-dependent manner, while overexpression of miR-494 increased miR-494 expression (Fig. 4A). In addition, ALP activity and ARS staining assays demonstrated that overexpression of miR-494 decreased ALP activity and mineralization of osteoblasts

(Fig. 4B, C). Moreover, we employed western blotting to confirm the inhibitory effect of miR-494 on osteogenic differentiation. The results showed that overexpression of miR-494 markedly reduced expression of RUNX2 and OSX (Fig. 4D), suggesting that miR-494 overexpression suppresses osteogenic differentiation. To extend our observations concerning the function of miR-494 in angiogenesis, we first transfected miR-494 mimics into MC3T3-E1 cells. As shown in Fig. 4E, miR-494 overexpression suppressed secretion of VEGFA, which was confirmed by ELISA. Then, HUVECs were exposed to the medium from MC3T3-E1 cells, which were treated with miR-494 mimics. As expected, overexpression of miR-494 dramatically inhibited the proliferation of HUVECs (Fig. 4F). In line with this finding, miR-494 overexpression not only restrained the migration of HUVECs but also reduced the formation of capillary tubes, implying that miR-494 restrains angiogenesis (Fig. 4G, H). In summary, these findings indicate that miR-494 inhibits angiogenesis and osteogenic differentiation.

SP1 overexpression or miR-494 inhibition attenuates the inhibition of sh-MALAT1 on angiogenesis and osteogenic differentiation

To further verify whether SP1 and miR-494 are involved in the regulation of MALAT1 in angiogenesis and osteogenic differentiation, we cotransfected MC3T3-E1 cells with MALAT1 shRNA and overexpression of SP1 plasmid or miR-494 inhibitor. As shown in Fig. 5A, either SP1 overexpression or miR-494 inhibition markedly elevated ALP activity, which was reduced by MALAT1 downregulation. Similarly, MALAT1 silencing suppressed extracellular matrix calcification, which was rescued by SP1 overexpression and miR-494 inhibition (Fig. 5B). Consistent with these findings, MALAT1 shRNA repressed protein expression of the osteogenic-related proteins RUNX2, OSX, and the SP1/TLR2/BMP2 axis, while SP1 amplification and miR-494 reduction increased expression levels of these protein (Fig. 5C), suggesting that SP1
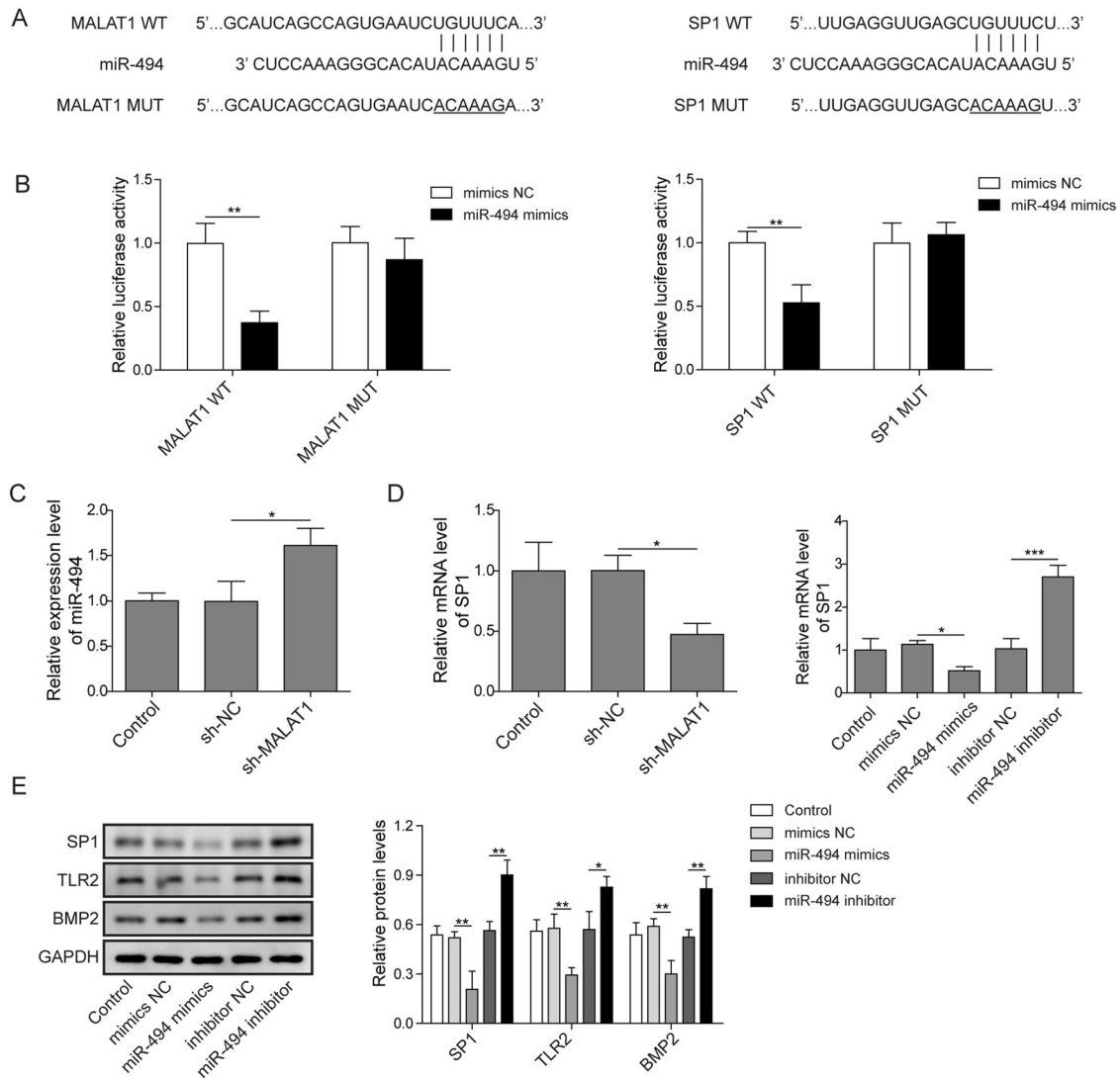
Fig. 3 MALAT1 mediates the SP1/TLR2/BMP2 axis by targeting miR-494. A Potential binding sites of miR-494 and MALAT1, miR-494 and SP1 were predicted using bioinformatics methods. **B** The luciferase activity was examined using a dual luciferase reporter assay. **C** Expression levels of miR-494 in MC3T3-E1 cells transfected with or without MALAT1 shRNA were detected by qRT-PCR. **D** mRNA expression of SP1 was assessed by qRT-PCR. **E** Protein expression of SP1, TLR2, and BMP2 was determined by western blot assay. Data are the mean ± SD of three separate experiments. The P value was determined by ANOVA following Tukey's post hoc test or Student's t-test. $*P < 0.05$, $**P < 0.01$, and $***P < 0.001$.

overexpression or miR-494 knockdown rescues the inhibition of osteogenic differentiation induced by MALAT1 depletion. Next, we analyzed the role of SP1 and miR-494 in the progression of angiogenesis induced by MALAT1. ELISA results demonstrated that silencing MALAT1 suppressed the secretion of VEGFA in MC3T3-E1 cells, which was subsequently eliminated by SP1 overexpression and miR-494 silencing (Fig. 5D). Next, HUVECs were incubated with supernatant from MC3T3-E1 cells that were cotransfected with MALAT1 shRNA and pcDNA-SP1 plasmid or miR-494 inhibitor. As shown in Fig. 5E, depletion of MALAT1 inhibited the survival of HUVECs, while SP1 overexpression and miR-494 inhibition enhanced the growth of HUVECs. In addition, Transwell assays and tube formation assays revealed that MALAT1 knockdown reduced the migration and tube formation potency of HUVECs, and these phenotypes were reversed by SP1 over-expression and miR-494 inhibition (Fig. 5F, G). Taken together, these results suggest that the inhibitory effect on angiogenesis triggered by MALAT1 depletion is rescued by SP1 overexpression or miR-494 knockdown.

DISCUSSION
During bone healing, blood vessels not only regulate the transport of CSCs, oxygen, nutrients, and metabolites but also produce autocrine signals involved in bone growth and homeostasis[28,29]. Hence, the coupling of angiogenesis and osteogenesis has a fundamental impact on the efficacy of bone regeneration[30,31]. Numerous studies have focused on the joint application of pro-osteogenic factors and pro-angiogenic factors that induce bone regeneration, indicating the therapeutic effect of bone defect repair[32]. Thus, it is urgent to investigate the molecular mechanisms participating in both angiogenesis and osteogenic differentiation of osteoblasts. In this study, we identified MALAT1 as a crucial regulator of angiogenesis and osteogenic differentiation and identified the entire regulatory signaling axis.

Numerous studies have indicated that MALAT1 promotes angiogenesis in diabetic retinopathy[33] and cardiovascular diseases[34,35], mostly in various cancers[11,36]. Li et al. showed that in gastric cancer, MALAT1 triggers tumorigenesis and metastasis by promoting vasculogenic mimicry and angiogenesis[11]. Sun et al.
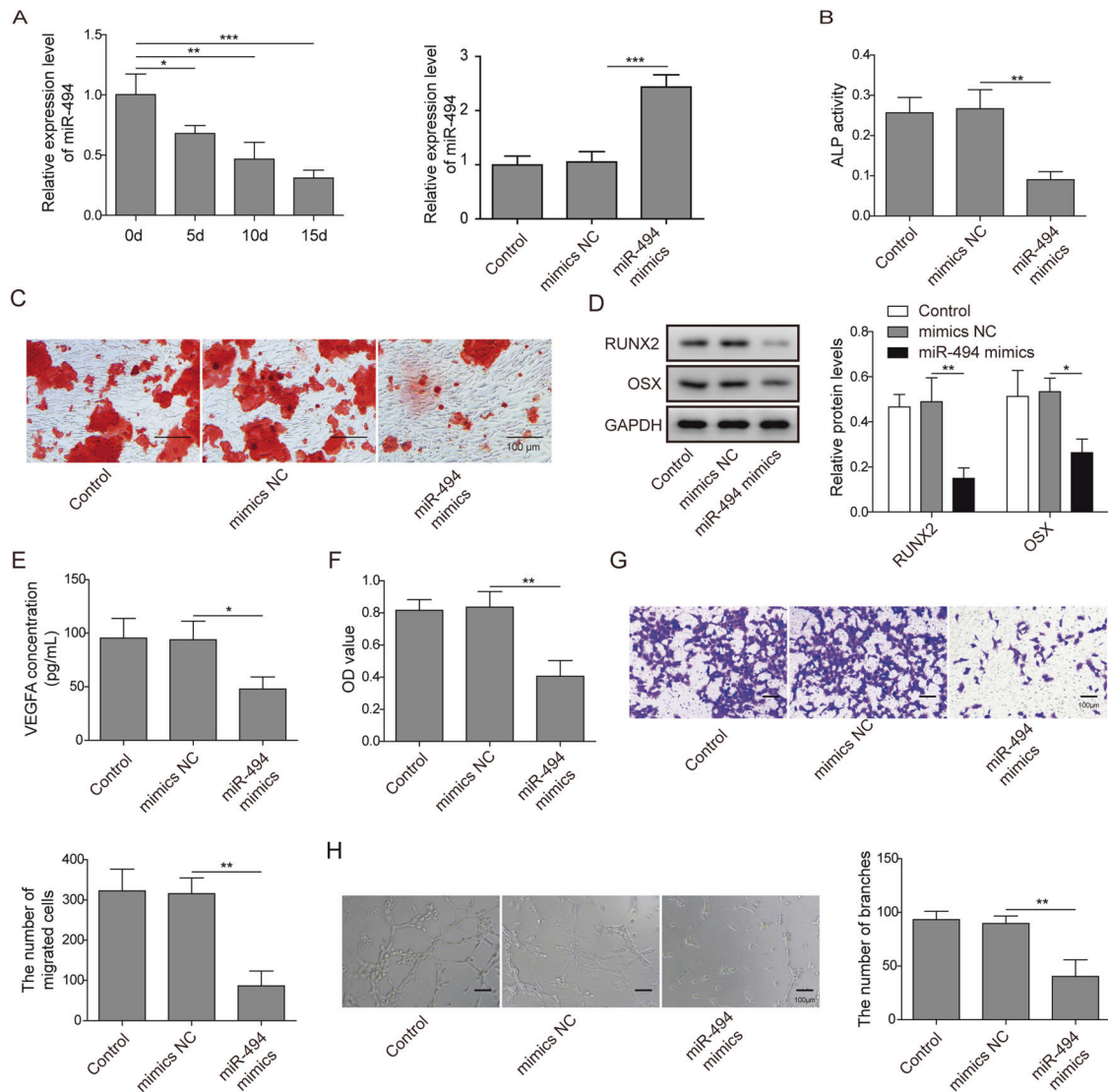
Fig. 4 MiR-494 overexpression inhibits angiogenesis and osteogenic differentiation. A Expression levels of miR-494 were evaluated by qRT-PCR. **B–E** MC3T3-E1 cells were transfected with miR-494 mimics or NC mimics. **B** Activity of ALP was detected using an ALP detection kit. **C** ARS assay was performed to assess mineralized nodules. **D** The protein expression of RUNX2 and OSX was determined by western blotting. **E** VEGFA concentrations in the supernatant were determined by ELISA. **F–H** HUVECs were treated with the supernatant from MC3T3-E1 cells transfected with miR-494 mimics or NC mimics. **F** Proliferation of HUVECs was detected by MTT assay. **G** Migration of HUVECs was measured using Transwell assays. **H** Tube size and numbers of HUVECs were observed under a microscope and imaged. Data are the mean ± SD for three separate experiments. The P value was determined by ANOVA following Tukey's post hoc test and Student's t-test. *$P < 0.05$, **$P < 0.01$, and ***$P < 0.001$.

demonstrated that the yes-associated protein 1-MALAT1-miR-126-5p signaling axis regulates angiogenesis and epithelial-mesenchymal transition in colorectal cancer[36]. In addition, a recent study revealed that MALAT1 induces Runx2-mediated osteogenic differentiation by targeting miR-30[12]. In this study, we discovered that knockdown of MALAT1 inhibits osteogenic differentiation, as ALP activity, mineralized nodules, and osteo-differentiated marker expression were restrained. In addition, knockdown of MALAT1 inhibited angiogenesis, since proliferation, migration, and capillary tube formation were blocked. These results showed that MALAT1 plays an important role in bone regeneration.

MiRNAs are widely reported to be involved in bone regeneration, angiogenesis, or both processes[37–39]. Fröhlich et al. demonstrated that miRNAs at the interface between osteogenesis and angiogenesis were bone regeneration targets[37]. MiR-494 was indicated to participate in angiogenesis[40,41]. Mao et al.

revealed that miR-494 promotes angiogenesis in lung cancer[40]. Asuthkar et al. showed a relationship between miR-494 and irradiation-induced angiogenesis[41]. Few studies have demonstrated the correlation between miR-494 and bone regeneration. The miRNA microarray results revealed that miR-494 is elevated in Bio-Oss, which is widely used in bone regeneration[42]. This study is the first to identify the role of miR-494 in regulating angiogenesis during bone regeneration. We found that overexpression of miR-494 inhibits both angiogenesis and osteogenic differentiation. Moreover, we are the first to report miR-494 as a direct target of MALAT1 by luciferase assay, enriching the regulatory mechanism connecting angiogenesis and osteogenic differentiation.

Recently, SP1 was uncovered as a key player in both angiogenesis and osteogenesis[43]. SP1 improves angiogenesis in preosteoblasts by stimulating the transforming growth factor-β1 (TGF-β1)/small mothers against decapentaplegic homolog 2
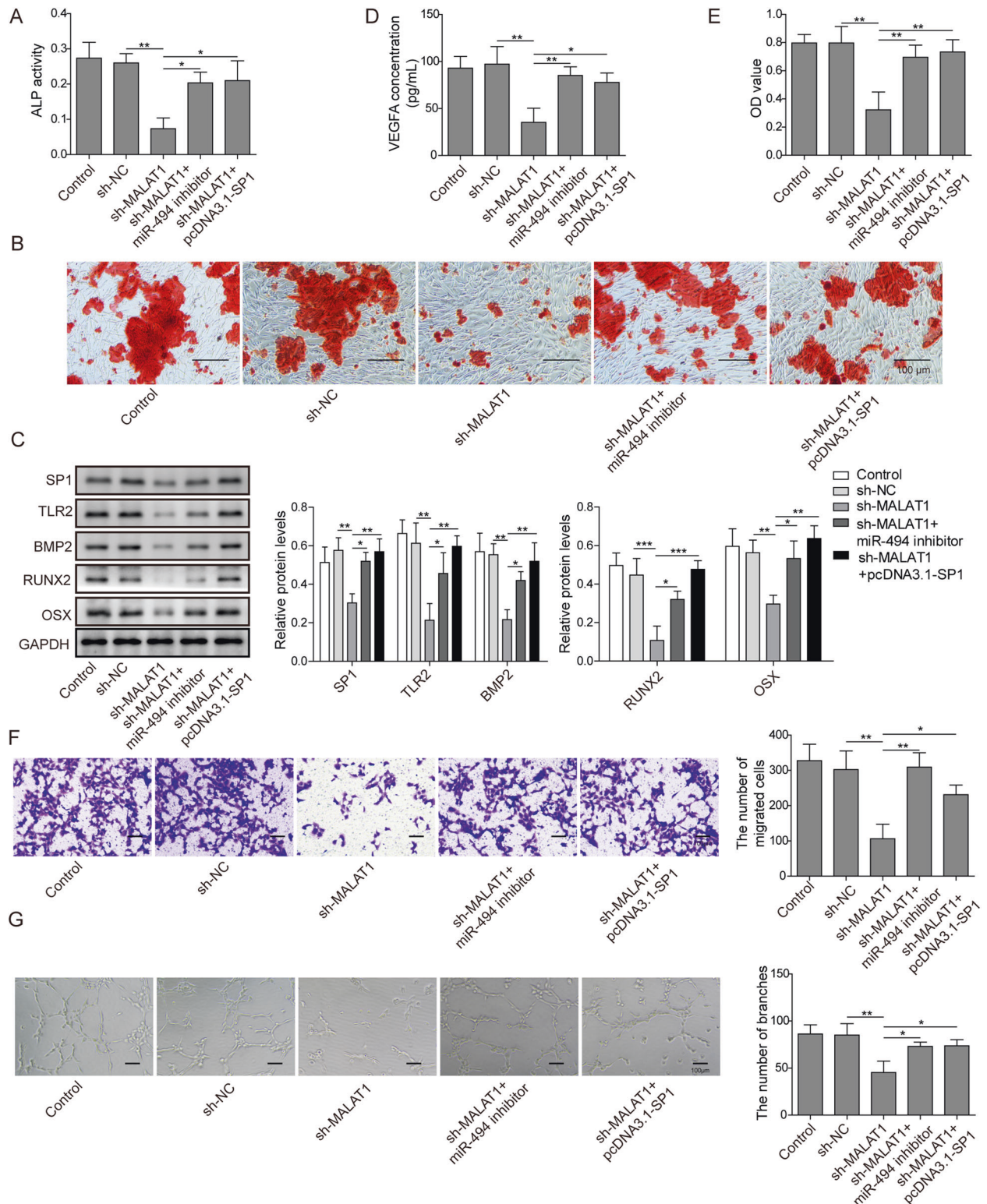
Fig. 5 SP1 overexpression or miR-494 knockdown attenuates the inhibition of sh-MALAT1 on angiogenesis and osteogenic differentiation. MC3T3-E1 cells were cotransfected with MALAT1 shRNA and miR-494 inhibition or SP1 overexpression plasmid. **A** The activity of ALP was detected using an ALP detection kit. **B** An ARS assay was performed to assess mineralized nodules. **C** Protein expression of SP1, TLR2, BMP2, RUNX2, and OSX was determined by western blotting. **D** The VEGFA concentrations in the supernatant were evaluated by ELISA. **E–G** HUVECs were treated with the supernatant from MC3T3-E1 cells. **E** Proliferation of HUVECs was detected by MTT assay. **F** Migration of HUVECs was measured by Transwell assays. **G** Tube formation of HUVECs in each well was observed under a microscope and then imaged. Data are the mean ± SD for three separate experiments. The *P* value was determined by ANOVA following Tukey's post hoc test or Student's *t*-test. **P* < 0.05, ***P* < 0.01, and ****P* < 0.001.

(SMAD2) pathway and increasing secretion of VEGF[43]. In addition, silencing SP1 reduces the expression of osteogenic-related proteins, including ALP, RUNX2, collagen 1A1, and osteocalcin, and inhibits ALP and ARS[44]. In this study, we also found that SP1 enhances both angiogenesis and osteogenic differentiation. However, the relationship between SP1 and MALAT1 or miR-494 is unclear. Recently, accumulating data have revealed that SP1 is an important transcription factor regulating lncRNA expression[45,46]. Huang et al. reported that SP1 connects with SP3 to promote MALAT1 expression in human hepatocellular carcinoma[47]. However, Li et al. showed that MALAT1 interacts with the SP1 protein and promotes transcriptional regulation of SP1 target genes in lung adenocarcinoma cells[19]. These findings suggest that the regulatory mechanism of MALAT1 and SP1 may be bidirectional. In this study, we found that MALAT1 promotes SP1 and its target genes by regulating miR-494. We are the first to demonstrate that SP1 is a target gene of miR-494 that subsequently induces SP1 downregulation. Moreover, we showed that SP1 overexpression or miR-494 knockdown rescues the inhibition of MALAT1 depletion on angiogenesis and osteogenic differentiation. Dunzendorfer et al. reported that SP1 binds to the TLR2 promoter, which is required for TLR2 expression[24]. Zhou et al. demonstrated that in response to peptidoglycan stimulation, expression of HIF-1α, VEGF, and BMP2 is increased in TLR2-modified BMSCs[23]. In this study, we also observed that SP1 mediates TLR2 and regulates BMP2 expression and that TLR2 enhances expression of BMP2. However, all the experiments were conducted under normoxic conditions, in which HIF-1α is ubiquitinated or degraded; thus, HIF-1α was not observed in this study. Overall, we are the first to identify the SP1/TLR2/BMP2 axis and the biological function of this signaling pathway.

VEGF plays a crucial role in vascular development and angiogenesis and influences skeletal development and postnatal bone repair, including the phases of inflammation, endochondral ossification, intramembranous ossification during callus formation, and bone remodeling[48]. Different mechanisms underlying the effects of VEGF on osteoblast function, including paracrine, autocrine and intracrine signaling during bone repair, have been discovered. VEGF plays an essential role in the coupling of angiogenesis and osteogenesis. When exposed to hypoxia during inflammation, osteoblasts release VEGF through the HIF-1α pathway, resulting in the activation of endothelial cells and the promotion of vessel permeability in mice[49]. In addition, osteogenic factors, such as BMP2, that are released from blood vessels promote osteoblast differentiation and mineralization in mice[50]. In turn, maturing osteoblasts generate angiogenic factors, such as platelet-derived growth factor and VEGF, to further support angiogenesis. In addition, SP1 promotes TGF-β1 expression, activates the SMAD2 pathway, and induces VEGF secretion, which enhanced angiogenic processes in MC3T3-E1 preosteoblast cells[43]. The above reports are in line with our findings. We also observed that VEGF is regulated by the SP1/TLR2/BMP2 signaling pathway. However, the following are limitations to this study: (i) lack of in vivo experiments and (ii) the relationship between VEGF and angiogenesis during the process of bone regeneration needs more exploration.

Taken together, this study demonstrated that MALAT1 enhances angiogenesis and osteogenic differentiation by targeting miR-494 and activating the SP1/TLR2/BMP2 signaling pathway, suggesting a novel regulatory signaling pathway for bone regeneration therapy.

DATA AVAILABILITY
All data generated or analyzed during this study are included in this published article.

REFERENCES
1. Quan, H. et al. LncRNA-AK131850 sponges MiR-93-5p in newborn and mature osteoclasts to enhance the secretion of vascular endothelial growth factor a promoting vasculogenesis of endothelial progenitor cells. Cell. Physiol. Biochem. 46, 401–417 (2018).
2. Almubarak, S. et al. Tissue engineering strategies for promoting vascularized bone regeneration. Bone 83, 197–209 (2016).
3. Yu, X., Tang, X., Gohil, S. V. & Laurencin, C. T. Biomaterials for bone regenerative engineering. Adv. Healthc. Mater. 4, 1268–1285 (2015).
4. Butler, J. M., Kobayashi, H. & Rafii, S. Instructive role of the vascular niche in promoting tumour growth and tissue repair by angiocrine factors. Nat. Rev. Cancer 10, 138–146 (2010).
5. Grosso, A. et al. It takes two to tango: coupling of angiogenesis and osteogenesis for bone regeneration. Front. Bioeng. Biotechnol. 5, 68 (2017).
6. Wang, C., Qu, Y., Suo, R. & Zhu, Y. Long non-coding RNA MALAT1 regulates angiogenesis following oxygen-glucose deprivation/reoxygenation. J. Cell. Mol. Med. 23, 2970–2983 (2019).
7. Zhang, S. Z. et al. STEEL participates in fracture healing through upregulating angiogenesis-related genes by recruiting PARP 1. Eur. Rev. Med. Pharmacol. Sci. 22, 3669–3675 (2018).
8. Kondo, A. et al. Long noncoding RNA JHDM1D-AS1 promotes tumor growth by regulating angiogenesis in response to nutrient starvation. Mol. Cell. Biol. 37, e00125–17 (2017). https://doi.org/10.1128/MCB.00125-17.
9. Wang, Y. et al. Long noncoding RNA H19 mediates LCoR to impact the osteogenic and adipogenic differentiation of mBMSCs in mice through sponging miR-188. J. Cell. Physiol. 233, 7435–7446 (2018).
10. Su, W., Xie, W., Shang, Q. & Su, B. The long noncoding RNA MEG3 is down-regulated and inversely associated with VEGF levels in osteoarthritis. Biomed. Res. Int. 2015, 356893 (2015).
11. Li, Y. et al. Long non-coding RNA MALAT1 promotes gastric cancer tumorigenicity and metastasis by regulating vasculogenic mimicry and angiogenesis. Cancer Lett. 395, 31–44 (2017).
12. Yi, J., Liu, D. & Xiao, J. LncRNA MALAT1 sponges miR-30 to promote osteoblast differentiation of adipose-derived mesenchymal stem cells by promotion of Runx2 expression. Cell Tissue Res. 376, 113–121 (2019).
13. Thomas, M., Lieberman, J. & Lal, A. Desperately seeking microRNA targets. Nat. Struct. Mol. Biol. 17, 1169–1174 (2010).
14. Hosseinpour, S., He, Y., Nanda, A. & Ye, Q. MicroRNAs involved in the regulation of angiogenesis in bone regeneration. Calcif. Tissue Int. 105, 223–238 (2019).
15. Sun, L. L., Li, W. D., Lei, F. R. & Li, X. Q. The regulatory role of microRNAs in angiogenesis-related diseases. J. Cell. Mol. Med. 22, 4568–4587 (2018).
16. Yang, C. et al. miRNA-21 promotes osteogenesis via the PTEN/PI3K/Akt/HIF-1alpha pathway and enhances bone regeneration in critical size defects. Stem Cell Res. Ther. 10, 65 (2019).
17. Qin, W. et al. Mir-494 inhibits osteoblast differentiation by regulating BMP signaling in simulated microgravity. Endocrine 65, 426–439 (2019).
18. Beishline, K. & Azizkhan-Clifford, J. Sp1 and the 'hallmarks of cancer'. FEBS J. 282, 224–258 (2015).
19. Li, S. et al. Long non-coding RNA metastasis-associated lung adenocarcinoma transcript 1 promotes lung adenocarcinoma by directly interacting with specificity protein 1. Cancer Sci. 109, 1346–1356 (2018).
20. Ko, D. & Kim, S. Cooperation between ZEB2 and Sp1 promotes cancer cell survival and angiogenesis during metastasis through induction of survivin and VEGF. Oncotarget 9, 726–742 (2018).
21. Aplin, A. C. et al. Regulation of angiogenesis, mural cell recruitment and adventitial macrophage behavior by Toll-like receptors. Angiogenesis 17, 147–161 (2014).
22. West, X. Z. et al. Oxidative stress induces angiogenesis by activating TLR2 with novel endogenous ligands. Nature 467, 972–976 (2010).
23. Zhou, Q. et al. The use of TLR2 modified BMSCs for enhanced bone regeneration in the inflammatory micro-environment. Artif. Cells Nanomed. Biotechnol. 47, 3329–3337 (2019).
24. Dunzendorfer, S., Lee, H. K. & Tobias, P. S. Flow-dependent regulation of endothelial Toll-like receptor 2 expression through inhibition of SP1 activity. Circ. Res. 95, 684–691 (2004).
25. Muramatsu, F., Kidoya, H., Naito, H., Sakimoto, S. & Takakura, N. microRNA-125b inhibits tube formation of blood vessels through translational suppression of VE-cadherin. Oncogene 32, 414–421 (2013).
26. Chen, C. et al. MiR-503 regulates osteoclastogenesis via targeting RANK. J. Bone Miner. Res. 29, 338–347 (2014).
27. Chen, Y. X., Huang, C., Duan, Z. B., Xu, C. Y. & Chen, Y. Klotho/FGF23 axis mediates high phosphate-induced vascular calcification in vascular smooth muscle cells via Wnt7b/beta-catenin pathway. Kaohsiung. J. Med. Sci. 35, 393–400 (2019).

28. Yu, W. L. et al. Enhanced osteogenesis and angiogenesis by mesoporous hydroxyapatite microspheres-derived simvastatin sustained release system for superior bone regeneration. *Sci. Rep.* **7**, 44129 (2017).
29. Li, S. et al. Supercritical CO_2 foamed composite scaffolds incorporating bioactive lipids promote vascularized bone regeneration via Hif-1alpha upregulation and enhanced type H vessel formation. *Acta Biomater.* **94**, 253–267 (2019).
30. Lovett, M., Lee, K., Edwards, A. & Kaplan, D. L. Vascularization strategies for tissue engineering. *Tissue Eng. Part B Rev.* **15**, 353–370 (2009).
31. Barabaschi, G. D., Manoharan, V., Li, Q. & Bertassoni, L. E. Engineering pre-vascularized scaffolds for bone regeneration. *Adv. Exp. Med. Biol.* **881**, 79–94 (2015).
32. Gotz, W., Reichert, C., Canullo, L., Jager, A. & Heinemann, F. Coupling of osteogenesis and angiogenesis in bone substitute healing – a brief overview. *Ann. Anat.* **194**, 171–173 (2012).
33. Liu, P. et al. LncRNA-MALAT1 promotes neovascularization in diabetic retinopathy through regulating miR-125b/VE-cadherin axis. *Biosci. Rep.* **39**, BSR20181469 (2019). https://doi.org/10.1042/BSR20181469.
34. Simion, V., Haemmig, S. & Feinberg, M. W. LncRNAs in vascular biology and disease. *Vascul. Pharmacol.* **114**, 145–156 (2019).
35. Uchida, S. & Dimmeler, S. Long noncoding RNAs in cardiovascular diseases. *Circ. Res.* **116**, 737–750 (2015).
36. Sun, Z. et al. YAP1-induced MALAT1 promotes epithelial-mesenchymal transition and angiogenesis by sponging miR-126-5p in colorectal cancer. *Oncogene* **38**, 2627–2644 (2019).
37. Frohlich, L. F. Micrornas at the interface between osteogenesis and angiogenesis as targets for bone regeneration. *Cells* **8**, 121 (2019). https://doi.org/10.3390/cells8020121.
38. Chen, X. et al. Identifying and targeting angiogenesis-related microRNAs in ovarian cancer. *Oncogene* **38**, 6095–6108 (2019).
39. Xie, Q. et al. Effects of miR-146a on the osteogenesis of adipose-derived mesenchymal stem cells and bone regeneration. *Sci. Rep.* **7**, 42840 (2017).
40. Mao, G. et al. Tumor-derived microRNA-494 promotes angiogenesis in non-small cell lung cancer. *Angiogenesis* **18**, 373–382 (2015).
41. Asuthkar, S. et al. Irradiation-induced angiogenesis is associated with an MMP-9-miR-494-syndecan-1 regulatory loop in medulloblastoma cells. *Oncogene* **33**, 1922–1933 (2014).
42. Palmieri, A. et al. Anorganic bovine bone (Bio-Oss) regulates miRNA of osteoblast-like cells. *Int. J. Periodontics Restorative Dent.* **30**, 83–87 (2010).
43. Ding, A., Bian, Y. Y. & Zhang, Z. H. SP1/TGFbeta1/SMAD2 pathway is involved in angiogenesis during osteogenesis. *Mol. Med. Rep.* **21**, 1581–1589 (2020).
44. Xia, C. P. et al. Sp1 promotes dental pulp stem cell osteoblastic differentiation through regulating noggin. *Mol. Cell. Probes* **50**, 101504 (2020).
45. Wang, Z. Q. et al. Long noncoding RNA UCA1 induced by SP1 promotes cell proliferation via recruiting EZH2 and activating AKT pathway in gastric cancer. *Cell Death Dis.* **8**, e2839 (2017).
46. Wang, Z. Q. et al. SP1-induced upregulation of the long noncoding RNA TINCR regulates cell proliferation and apoptosis by affecting KLF2 mRNA stability in gastric cancer. *Oncogene* **34**, 5648–5661 (2015).
47. Huang, Z. et al. Sp1 cooperates with Sp3 to upregulate MALAT1 expression in human hepatocellular carcinoma. *Oncol. Rep.* **34**, 2403–2412 (2015).
48. Hu, K. & Olsen, B. R. The roles of vascular endothelial growth factor in bone repair and regeneration. *Bone* **91**, 30–38 (2016).
49. Wang, Y. et al. The hypoxia-inducible factor alpha pathway couples angiogenesis to osteogenesis during skeletal development. *J. Clin. Invest.* **117**, 1616–1626 (2007).
50. Matsubara, H. et al. Vascular tissues are a primary source of BMP2 expression during bone formation induced by distraction osteogenesis. *Bone* **51**, 168–180 (2012).

AUTHOR CONTRIBUTIONS

FUNDING

COMPETING INTERESTS

The authors declare no competing interests.

ETHICS APPROVAL AND CONSENT TO PARTICIPATE

Because all the experiments were conducted in cells, no ethical approval was needed.

ADDITIONAL INFORMATION

Correspondence and requests for materials should be addressed to Z.-H.Z.

Reprints and permission information is available at http://www.nature.com/reprints

Publisher's note Springer Nature remains neutral with regard to jurisdictional claims in published maps and institutional affiliations.